Control of Thermophysical Properties of Langasite-Type La3Ta0.5Ga5.5O14 Crystals for Pressure Sensors

Haruki Usui, Makoto Tokuda, Kazumasa Sugiyama, Takuya Hoshina, Takaaki Tsurumi, Kheirreddine Lebbou, Ikuo Yanase, Hiroaki Takeda

HAL Id: hal-03011177
https://hal.science/hal-03011177

Submitted on 18 Nov 2020

Control of Thermophysical Properties of Langasite-Type $La_3Ta_{0.5}Ga_{5.5}O_{14}$ Crystals for Pressure Sensors

Haruki Usui [1], Makoto Tokuda [2], Kazumasa Sugiyama [2], Takuya Hoshina [1], Takaaki Tsurumi [1], Kheirreddine Lebbou [3], Ikuo Yanase [4] and Hiroaki Takeda [1,4,*]

[1] School of Materials and Chemical Technology, Tokyo Institute of Technology, Meguro, Tokyo 152-8552, Japan; usui.h.ab@m.titech.ac.jp (H.U.); thoshina@ceram.titech.ac.jp (T.H.); ttsurumi@ceram.titech.ac.jp (T.T.)

[2] Institute for Materials Research (IMR), Tohoku University, Sendai 980–8577, Japan; tokuda@imr.tohoku.ac.jp (M.T.); kazumasa@imr.tohoku.ac.jp (K.S.)

[3] Institut Lumière Matière, UMR5306 CNRS, Universite de Lyon 1, 69622 Villeurbanne CEDEX, France; kheirreddine.lebbou@univ-lyon1.fr

[4] Graduate School of Science and Engineering, Saitama University, 255 Shimo-Okubo, Sakura-ku, Saitama 338-8570, Japan; yanase@apc.saitama-u.ac.jp

* Correspondence: takeda@apc.saitama-u.ac.jp; Tel.: +81-48-858-3501

check for updates

Abstract: We present a possible method to reduce the anisotropy of the thermal stress generated on langasite-type $La_3Ta_{0.5}Ga_{5.5}O_{14}$ (LTG) piezoelectric crystals arising from the mismatch of the thermal expansion coefficients and Young's moduli of the crystals and metals at high temperatures. To formulate this method, the thermal stresses of order-type langasite crystals, in which each cation site is occupied by one element only, were calculated and compared to each other. Our results suggest that the largest cation site affects the thermal stress. We attempted to replace La^{3+} in LTG by a larger ion and considered Sr^{2+}. Single crystals of strontium-substituted LTG (Sr-LTG) were grown using the Czochralski method. The thermal stress along the crystallographic *c*-axis decreased but that perpendicular to the *c*-axis increased by strontium substitution into the LTG crystal. The anisotropic thermal stress was reduced effectively. The Sr-LTG single crystal is a superior candidate material for pressure sensors usable at high temperatures.

Keywords: anisotropy; thermal stress; langasite; pressure sensor; substitution

1. Introduction

In recent years, the automobile industry has been faced with a number of environmental and energy problems. Consequently, improvements to fuel efficiency and reduction in exhaust gas have been required [1]. Combustion pressure sensors are attractive devices for improving the combustion efficiency of engines. Such devices are directly placed in engine cylinders and combustion efficiency is improved by feedback control of the fuel injection based on data of the combustion pressure changes in the cylinder. An engine with a combustion pressure sensor can reduce NOx emissions by approximately 30%, and the emission of CO_2, which is a cause of global warming, by about 10% [2].

$La_3Ga_5SiO_{14}$ (langasite) family single crystals are attractive piezoelectric materials for use in combustion pressure sensors because they show no phase transitions up to their melting temperature and can be easily grown to large sizes using the Czochralski (Cz) technique [3–9]. $GaPO_4$ crystals [10] and rare-earth (Re) calcium oxoborate $ReCa_4O(BO_3)_3$ crystals [11] have also been reported to be promising candidates because the former has a high phase transition temperature of 930 °C and the latter maintains the piezoelectric property to its melting temperature of approximately 1600 °C.

However, bulk growth of $GaPO_4$ crystals is very difficult [12], while $ReCa_4O(BO_3)_3$ crystals have very low crystal symmetries (monoclinic *m*), and then show pyroelectricity [13]. Recently, gehlenite $Ca_2Al_2SiO_7$ and related crystals in the melilite group have been the subject of much study, because they exhibit piezoelectricity without any accompanying pyroelectricity [14,15]. The crystals also have very clear cleavage planes, which is a matter of concern for target applications in combustion pressure sensors.

Among the langasite family crystals, the $La_3Ta_{0.5}Ga_{5.5}O_{14}$ (LTG) single crystal is the most promising candidate [16,17] because it shows weak temperature dependence of its piezoelectric properties, and high electrical resistivity at high temperatures. Fracture of the crystal element during use is a matter of concern for combustion pressure sensors [18]. The fractures can be attributed to the high impulsive force generated during abnormal combustion. During use, thermal stresses along and perpendicular to the crystallographic *c*-axis are anisotropically generated at a working temperature of approximately 200 °C. At high temperatures, anisotropic thermal stress is caused by the difference in the thermal expansion coefficients and Young's moduli among the LTG crystals used as the substrate and the metals used as crystal support. Reducing the anisotropic thermal stress by applying element substitution into the LTG may be an effective way to avoid this phenomenon.

In this study, first, we describe the calculation of the thermal stress using the data of the linear thermal expansion coefficients and elastic stiffness coefficients instead of the Young's moduli, of four order-type langasite family crystals and the metal at high temperatures. Then, the candidate of the substituent element Sr was selected. We have also reported the effect of Sr substitution on the LTG crystals, which demonstrated a successful reduction in the anisotropic thermal stress.

2. Materials and Methods

2.1. Thermal Stress Calculation

A simplified structure surrounding the piezoelectric crystal substrate of the combustion pressure sensor was constructed for thermal stress calculation [19], as shown in Figure 1a. The piezoelectric *X*-cut of the crystal substrate and metal were in contact. The *X*-cut corresponds to the Miller plane $(1\bar{2}0)$ perpendicular to the crystallographic *a*-axis. The *a*- and *c*-axes correspond to the *x*- and *z*-axes, respectively. Langasite family crystals belong to a trigonal crystal system. Hence, the *y*-axis is the [120] direction. As the piezoelectric coefficient used in the combustion pressure sensor is d_{11}, the *x*-, *y*-, and *z*-axes are as indicated in Figure 1. At the initial state, the length of the crystal is the same as that of the metal. As the crystal is strongly fixed by the metal part, the crystal attempts to extend with the metal during temperature rise. Under the conditions shown in Figure 1b, the expansions of the crystal Δl_c and the metal Δl_m caused by their own thermal expansions are expressed using the following Equations (1) and (2):

$$\Delta l_c = \alpha_c \Delta T l_0, \tag{1}$$

$$\Delta l_m = \alpha_m \Delta T l_0, \tag{2}$$

where α_c and α_m are the linear thermal expansion coefficients (LTEC) of crystal and metal, respectively. ΔT is the change in temperature and l_0 is the length of both the crystal and metal at the initial temperature. As the metal is composed of polycrystals, α_m does not depend on the direction, that is, it is isotropic. However, there are two types of α_c (α_{11} and α_{33}) in langasite family crystals. In this study, α_{11} and α_{33} are defined as α_y ($=\alpha_x$) and α_z, respectively. It is assumed that the external force applied from the crystal to the metal is equal to that applied from the metal to the crystal, and this is defined as the thermal stress σ. The thermal stress generated between the crystal and the metal was calculated at 400 °C, which was the maximum working temperature. Stainless steel, composed of iron and carbon, is normally used for the metal, and its LTEC α_m is assumed to be 11×10^{-6} K^{-1} in the calculation [19]. The α_y and α_z values of the langasite family crystals were determined in this study. As both the crystal and metal were fixed, as shown in Figure 1c, both the crystal and metal tend to expand to the same

length during heating. Therefore, the elongation λ of the crystal and metal from room temperature (23 °C) to the working temperature is expressed using the following Equations (3) and (4):

$$\lambda = \Delta l_c + (\sigma/E_c)l_0, \tag{3}$$

$$\lambda = \Delta l_m + (-\sigma/E_m)l_0, \tag{4}$$

where E_c is the elastic stiffness of the crystal and E_m is the Young's modulus of the metal. In general, the LTEC of metals is larger than that of crystals. Therefore, the metal is stressed by the crystal in the negative direction, and the crystal is stressed in the opposite direction. Finally, the thermal stress σ can be calculated as:

$$\sigma = \frac{(\alpha_m - \alpha_c)E_m E_c}{(E_m + E_c)}\Delta T, \tag{5}$$

As mentioned above, anisotropic α_y and α_z should be considered, and we have treated two types of thermal stresses σ independent of each other. Therefore, σ_y and σ_z along the y and z directions of the crystal were calculated. In this study, the Young's modulus of the metal was determined to be 152 GPa [19]. The elastic stiffness coefficients (EFC) of the crystal were determined by electroacoustic method, as described later. The aim of this study was to determine the ratio of σ_y and σ_z of the LTG crystal, $\sigma_y/\sigma_z = 1$ by element substitution.
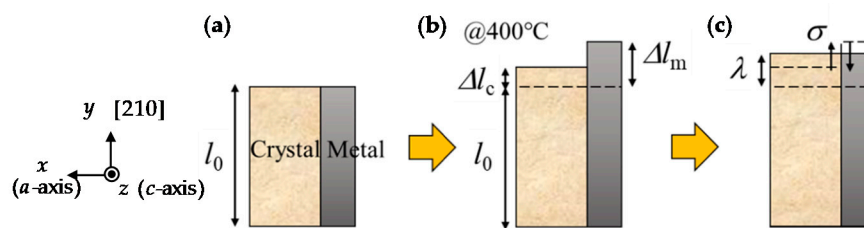

Figure 1. Schematic of the thermal stress calculation process. (**a**) Initial state of the device element; (**b**) Thermal expansion of the crystal and metal; (**c**) Generated thermal stress.

LTECs were obtained to investigate the thermal expansion anisotropy of order-type langasite family single crystals, as well as to calculate the thermal stress. The langasite-type crystals belong to the trigonal crystal system, point group 32, and space group *P*321. Thus, there are two independent expansion components, α_{11} and α_{33}, along the crystallographic *a*- and *c*-axes, respectively. The LTECs were calculated using changes in the lattice constants *a* and *c*. Measurements were performed using a powder X-ray diffraction (XRD) method (Rigaku Ultim III SS), with a high-temperature furnace attachment, in the temperature range 23 to 500 °C, at intervals of 100 °C. We used Al_2O_3 polycrystal powder as the standard. The LTECs α_{11} and α_{33} were calculated by the following:

$$\alpha_{11} = 1/a_0 \cdot \Delta a/\Delta T, \tag{6}$$

$$\alpha_{33} = 1/c_0 \cdot \Delta c/\Delta T, \tag{7}$$

where a_0 (c_0), Δa (Δc), and ΔT represent the initial lattice constant of the sample at room temperature and the displacements and temperature change, respectively. The values of α_{11} and α_{33} correspond to α_y and α_z in Figure 1, respectively. As mentioned later, the LTG crystals show high anisotropic thermal stress, that is, high ratio of α_y and α_z.

In the crystal structure of the langasite family, there are four types of cation sites, and the chemical formula can be represented as $A_3BC_3D_2O_{14}$. The corresponding crystal structure is schematically shown in Figure 2. *A* and *B* represent the decahedral and octahedral sites, respectively; *C* and *D* represent tetrahedral sites, with the *D* site being smaller than the *C* site. In the LTG crystal, La^{3+} occupies the *A* sites, Ta^{5+} occupies half of the *B* sites, and Ga^{3+} occupies another half of the *B* sites and both the *C* and *D* sites. The langasite family crystals are classified into two types depending on their site occupation

patterns [20]. One is known as a disorder-type structure (such as LGS and LTG), in which at least one of the four cation sites is occupied by two or more different elements (Ta and Ga in LTG). The other is known as an order-type structure (such as $Sr_3TaGa_3Si_2O_{14}$), in which all cation sites are occupied by a single element [21]. In this study, we measured the LTEC using $Ca_3TaGa_3Si_2O_{14}$ (CTGS) [22], $Ba_3TaGa_3Si_2O_{14}$ (BTGS) [23], $Ca_3NbGa_3Si_2O_{14}$ (CNGS) [24], and $Ca_3TaAl_3Si_2O_{14}$ (CTAS) [25] crystals. By comparing the thermal stress ratio α_y/α_z of each crystal, it was found that the four sites were effective in reducing the anisotropic thermal stress of the LTG crystal. The CTGS, BTGS, CNGS, and CTAS crystal ingots have been reported in other studies [22–25]. These crystals were pulverized and used for powder XRD. As mentioned later, we found that the largest cation *A* site affects the thermal stress. Then, we formulated an idea to replace La^{3+} in LTG by larger ions, such as Sr^{2+}. On the basis of this idea, we attempted to grow strontium-substituted LTG (Sr-LTG) single crystals.
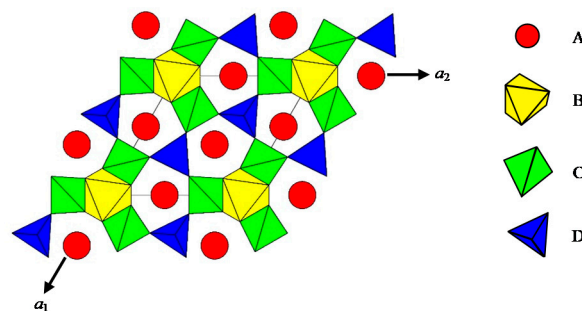

Figure 2. Schematic illustration of the langasite-type crystal structure viewed along the [001] direction.

2.2. Crystal Growth and Characterization

Sr-LTG crystals were grown using a conventional RF-heating Czochralski (Cz) technique. Stoichiometric amounts of oxides and carbonates with 99.99% purity, corresponding to $La_{2.9}Sr_{0.1}Ta_{0.55}Ga_{5.45}O_{14}$ (Sr-LTG) were prepared and calcined at 1300 °C, for 5 h, in air. The chemical composition of the Sr-LTG was selected based on a previous study [26]. An iridium crucible was used with a diameter and height of 50 mm. The calcined powder was charged into a crucible. The growth atmosphere was achieved by flowing argon gas at 10^{-3} m^3/min and oxygen gas at 10^{-5} m^3/min. A pure LTG single crystal bar was used as the seed. The pulling rate and rotation rates were 0.5 mm/h and 15 rpm, respectively. Phase identification of the as-grown crystals was performed by powder XRD. The crystal density was calculated using the lattice parameter, and the chemical composition was determined using an electron probe microanalyzer (EPMA).

In the Sr-LTG crystals, the independent material constants consisted of two dielectric, two piezoelectric, and six elastic compliance constants (ε_{ij}, d_{ij}, and s_{ij}, respectively). These material constants were determined using an impedance/gain phase analyzer (HP 4194A, Agilent) as reported previously [27,28]. The electromechanical coupling factor k_{ij} and the piezoelectric modulus were evaluated by measuring the mechanical series resonance frequency f_s and parallel resonance frequency f_p of the equivalent resonators. The equivalent resonators were fabricated in the form of plates according to the length-extensional vibration mode. The dielectric constants, ε_{ij}, were determined by measuring the capacitances of the resonators by considering the parasitic capacitance.

3. Results and Discussion

Figure 3 shows the temperature dependence of the lattice constants along the crystallographic *a*- and *c*-axes of the $Ba_3TaGa_3Si_2O_{14}$ (BTGS) crystal. These lattice constants changed linearly across the entire temperature range. The calculated LTEC of the *a*-axis was almost the same as that of the *c*-axis, as shown in Table 1. The LTECs at 400 °C were all positive, indicating that the LTEC of the BTGS crystal is anisotropic. To calculate the thermal stress for the langasite family crystals, the LTECs of $Ca_3TaGa_3Si_2O_{14}$, $Ca_3NbGa_3Si_2O_{14}$, $Ca_3TaAl_3Si_2O_{14}$, and $La_3Ta_{0.5}Ga_{5.5}O_{14}$ crystals were also measured

using the same process used for the BTGS crystal. All the LTECs and the elastic stiffness data are provided in Table 1 for the calculation of the thermal stresses.
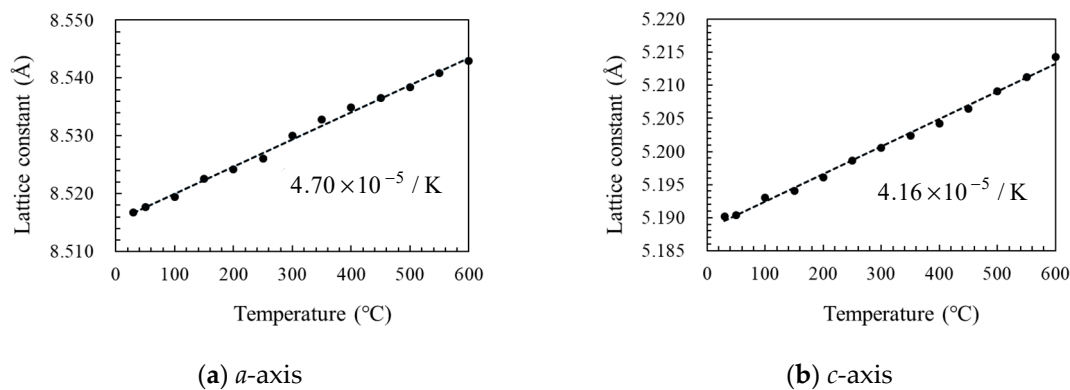

(a) *a*-axis

(b) *c*-axis

Figure 3. Dependence of the lattice constants on the temperature of the $Ba_3TaGa_3Si_2O_{14}$ crystal along the crystallographic (**a**) *a*-axis and (**b**) *c*-axis. Linear thermal expansion coefficients are also shown inside.

Table 1. Elastic stiffness coefficients (ESCs) and linear thermal expansion coefficients (LTECs) of the langasite family crystals. CTGS, BTGS, CNGS, CTAS, and LTG are the abbreviations for $Ca_3TaGa_3Si_2O_{14}$ [22], $Ba_3TaGa_3Si_2O_{14}$ [23], $Ca_3NbGa_3Si_2O_{14}$ [24], $Ca_3TaAl_3Si_2O_{14}$ [25], $La_3Ta_{0.5}Ga_{5.5}O_{14}$ [29], respectively.

Crystal	ESC (GPa)		TEC (10^{-6} K^{-1})	
	c_y	c_z	α_y	α_z
CTGS	123.2	178.1	8.30	7.13
BTGS	211.0	423.0	5.52	8.02
CNGS	155.0	226.0	8.02	7.70
CTAS	184.4	477.4	8.08	8.12
LTG	189.8	263.5	7.99	5.97

ESC were calculated using the data reported in [22–25,29].

Using the ESCs and LTECs in Table 1, the thermal stresses were calculated using Equation (5) and are presented in Figure 4. The thermal stress of the LTG crystal, the most promising candidate for the combustion pressure sensor, was also calculated. The data of the LTG crystal were calculated using the values reported in previous studies [29,30]. As σ_y was twice the σ_z value in the LTG crystal, the anisotropy of thermal stress was high. There are two possible methods to reduce the anisotropy of thermal stress in LTG crystals. One method is to increase σ_y, and the other method is to decrease σ_z. By comparing the σ_y of CTGS, BTGS, CNGS, and CTAS crystals, it was demonstrated that the *A* site ion with a higher ionic radius effectively increased the value of σ_y. However, as the σ_z values were the same in all the crystals used in this study, it was inferred that not all substituent elements led to a decrease in the σ_z of the LTG. Therefore, by substituting atoms with larger ionic radii for the *A* site, such as CTGS and BTGS, it was expected that the anisotropy of the thermal stress could be reduced by increasing σ_y. Bi^{3+} (1.17 Å), Na^+ (1.18 Å), Sr^{2+} (1.26 Å), Pb^{2+} (1.29 Å), and Ba^{2+} (1.42 Å) were possible candidates for ions with an ionic radius larger than that of La^{3+} (1.16 Å) [31]. The ionic radii of Bi^{3+} and Na^+ are almost the same as that of La, and the change in the anisotropy of the thermal stress should be small. Moreover, Pb^{2+} was excluded because of its toxicity, and Ba^{2+} was not considered because it is difficult to introduce Ba^{2+} into the LTG crystal lattice [26]. Therefore, in the present study, the growth of Sr-LTG single crystals was attempted based on a previous study [26].
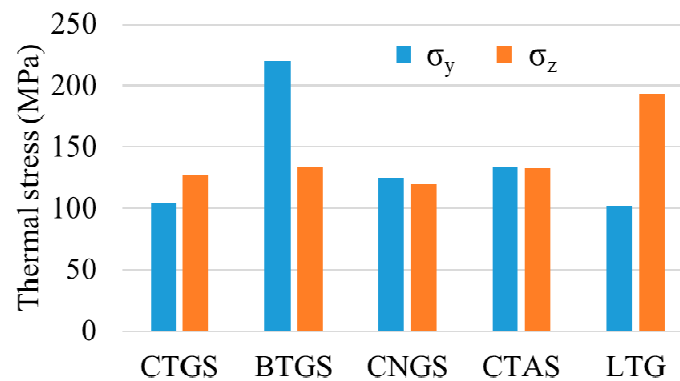
Figure 4. Thermal stress, σ_y and σ_z, of the langasite family crystals at 400 °C along the [120] (*y*-axis) and *c*-axis, respectively. The data were calculated using the elastic stiffness coefficients (ESCs), linear thermal expansion coefficients (LTECs) shown in Table 1. CTGS, BTGS, CNGS, CTAS, and LTG are the abbreviations for $Ca_3TaGa_3Si_2O_{14}$, $Ba_3TaGa_3Si_2O_{14}$, $Ca_3NbGa_3Si_2O_{14}$, $Ca_3TaAl_3Si_2O_{14}$, $La_3Ta_{0.5}Ga_{5.5}O_{14}$, respectively.

Growth of Sr-LTG crystals has been reported [26], and therefore the starting composition of Sr-LTG was set as $La_{2.9}Sr_{0.1}Ta_{0.55}Ga_{5.45}O_{14}$. The Sr-LTG single crystal without any inclusions was successfully grown by the Cz method, as shown in Figure 5. The Sr-LTG crystals grown, in this study, were transparent, orange in color, and 23 mm in diameter and 70 mm in length. The upper part of the boule contained six developed flat surfaces, which consisted of planes parallel to the <001> growth direction. Backscattering Laue X-ray analysis showed that the flat surfaces correspond to {100} planes. Small cracks and bubbles were observed in the lower part of the boule. All peaks of the crystal powder XRD patterns agreed with those of the LTG structure. We carefully eliminated these macro defects via proper sample preparation, including cutting and polishing, for material constant measurement. The solidification fraction, $g = W_{crystal}/W_{initial}$, where $W_{crystal}$ and $W_{initial}$ are the weights of the grown crystal and the starting melt, respectively, was 0.36. The Sr content of the LTG crystal was smaller than that of the starting raw materials, taking into account the accuracy of EPMA analysis conducted in this study. This result agrees well with that reported in [26]. The grown crystal was pulverized, and its powder was also used for measurement of LTEC.
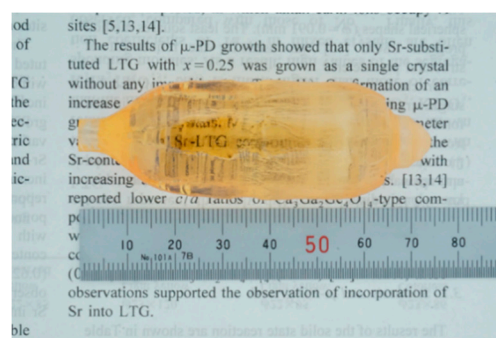

Figure 5. Photograph of side view of strontium-substituted LTG (Sr-LTG) crystals grown by the Czochralski (Cz) method.

The ESC and LTEC of the Sr-LTG crystal were measured, and the thermal stresses σ_y and σ_z were calculated and are listed in Table 2, along with those of the LTG crystal [29]. The ESCs, c_y and c_z, were higher and lower, respectively, for Sr-LTG than for LTG, indicating that the LTG crystal lattice was hardened along the direction perpendicular to the *c*-axis and softened along the *c*-axis, due to Sr substitution, respectively. The reasons for this should be clarified from the viewpoint of changes to crystal structure by Sr substitution. Detailed structural analysis is currently under investigation.

The thermal stresses, α_y and α_z, of the Sr-LTG crystal were higher and lower than those of the LTG crystal, respectively. Thus, the thermal stress ratio α_y/α_z of the Sr-LTG crystal was closer to unity than that of the LTG crystal. Consequently, the anisotropy of the thermal stress was effectively reduced by the Sr substitution into the LTG lattice. Electromechanical properties were characterized using the $(XYt)\theta°(\theta = 0, 30, 60,$ and $-30)$ substrates of the Sr-LTG crystals. The d_{11} values determined were 5.81 pC/N for the Sr-LTG. The magnitude of the piezoelectric d_{11} coefficient for Sr-LTG was lower than that for LTG (7.06 pC/N [32]). The reduction by Sr substitution has been previously reported [26]. The reason for this remains under consideration and will be clarified by combining the detailed crystal structural analysis and characterization of all the electromechanical coefficients. The d_{11} coefficient was still higher than the d_{11} values of quartz (2.30 pC/N [33]), and hence suggested that the Sr-LTG crystal is a superior candidate material for combustion pressure sensors.

Table 2. Elastic stiffness coefficients (ESCs), linear thermal expansion coefficients (LTECs), thermal stresses, and the ratio of LTG and Sr-LTG crystals.

Crystal	ESC (GPa)		LTEC (10^{-6} K^{-1})		Thermal Stress (MPa)		Ratio
	c_y	c_z	α_y	α_z	σ_y	σ_z	σ_y/σ_z
LTG [29,30]	189.8	263.5	7.99	5.97	101.9	193.9	0.53
Sr-LTG	206	214	7.80	6.43	112.2	162.5	0.69

4. Conclusions

In this study, we formulated a method to reduce the anisotropy of the thermal stress generated on LTG crystals when the LTG crystal was used as a combustion pressure sensor. This was achieved by comparing the anisotropy of the thermal stress of order-type langasite family crystals. The solution included the *A* site (La^{3+}) in the LTG crystal being substituted with the larger Sr^{2+} ions. Therefore, the crystal growth of Sr-LTG was undertaken using the Cz method. The Sr-LTG single crystal without any inclusions was successfully grown. By Sr substitution, the thermal stress ratio α_y/α_z of the LTG crystal was effectively reduced, while maintaining the piezoelectric property. We conclude that the Sr-LTG single crystal is a superior candidate material for pressure sensors usable at high temperatures.

Author Contributions: Conceptualization, H.T. and H.U.; methodology, H.T., H.U., M.T., K.S. and K.L.; software, T.H. and T.T.; writing—original draft preparation, H.T.; writing—review and editing, T.H., T.T. and I.Y.; funding acquisition, H.T. All authors have read and agreed to the published version of the manuscript.

References

1. Rogers, D.R. *Engine Combustion: Pressure Measurement and Analysis*; SAE International: Warrendale, PA, USA, 2010.
2. Tsukada, K.; Takeuchi, M.; Tokumitsu, S.; Ohmura, Y.; Kawaguchi, K. Combustion pressure sensor. *R&D Rev. Toyota CRDL* **1993**, *28*, 49–57. (In Japanese)
3. Shimamura, K.; Takeda, H.; Kohno, T.; Fukuda, T. Growth and characterization of lanthanum gallium silicate La$_3$Ga$_5$SiO$_{14}$ single crystals for piezoelectric application. *J. Cryst. Growth* **1996**, *163*, 388–392. [CrossRef]
4. Takeda, H.; Shimamura, K.; Kohno, T.; Fukuda, T. Growth and Characterization of La$_3$Nb$_{0.5}$Ga$_{5.5}$O$_{14}$ Single Crystals. *J. Cryst. Growth* **1996**, *169*, 503–508. [CrossRef]
5. Bohm, J.; Heimann, R.B.; Hengst, M.; Roewer, R.; Schindler, J. Czochralski growth and characterization of piezoelectric single crystals with langasite structure: La$_3$Ga$_5$SiO$_{14}$ (LGS), La$_3$Ga$_{5.5}$Nb$_{0.5}$O$_{14}$ (LGN), and La$_3$Ga$_{5.5}$Ta$_{0.5}$O$_{14}$ (LGT). Part I. *J. Cryst. Growth* **1999**, *204*, 128–136. [CrossRef]

6. Takeda, H.; Fukuda, T.; Kawanaka, H.; Onozato, N. Effect of starting melt composition on growth of $La_3Ta_{0.5}Ga_{5.5}O_{14}$ crystal. *J. Mater. Sci. Mater. Electron.* **2001**, *12*, 199–202. [CrossRef]

7. Uda, S.; Wang, S.Q.; Konishi, N.; Inaba, H.; Harada, J. Growth habits of 3 and 4-inch langasite single crystals. *J. Cryst. Growth* **2002**, *237*, 707–713. [CrossRef]

8. Boutahraoui, B.; Nehari, A.; Boy, J.J.; Vacheret, X.; Allani, M.; Cabane, H.; Dumortier, M.; Derbal, M.; Lebbou, K. LGT ($La_3Ga_{5.5}Ta_{0.5}O_{14}$) langatate bulk crystal grown from the melt by Czochralski technique and characterization. *Opt. Mater.* **2017**, *65*, 103–105. [CrossRef]

9. Allani, M.; Batis, N.; Laroche, T.; Nehari, A.; Cabane, H.; Lebbou, K.; Vacheret, X.; Boy, J.J. Effects of the Langatate crystal quality on the resonance frequency stability of bulk acoustic wave resonators. *Adv. Appl. Ceram.* **2018**, *117*, 279–284. [CrossRef]

10. Krempl, P.; Schleinzer, G.; Wallnöfer, W. Gallium phosphate, $GaPO_4$: A new piezoelectric crystal material for high-temperature sensorics. *Sens. Actuators A Phys.* **1997**, *61*, 361–363. [CrossRef]

11. Yu, F.; Zhang, S.; Zhao, X.; Yuan, D.; Qin, L.; Wang, Q.-M.; Shrout, T.R. Dielectric and electromechanical properties of rare earth calcium oxyborate piezoelectric crystals at high temperatures. *IEEE Trans. Ultra. Ferro. Freq. Contr.* **2011**, *58*, 868–873.

12. Balitsky, D.V.; Philippot, E.; Papet, P.; Balitsky, V.S.; Pey, F. Comparative crystal growth of $GaPO_4$ crystals in the retrograde and direct solubility range by hydrothermal methods of temperature gradient. *J. Cryst. Growth* **2005**, *275*, e887–e894. [CrossRef]

13. Takeda, H.; Sako, H.; Shimizu, H.; Kodama, K.; Nishida, M.; Nakao, H.; Nishida, T.; Okamura, S.; Shikida, T.; Shiosaki, T. Growth and characterization of lanthanum Calcium Oxoborate $LaCa_4O(BO_3)_3$ single crystals. *Jpn. J. Appl. Phys.* **2003**, *42*, 6081–6085. [CrossRef]

14. Takeda, H.; Hagiwara, M.; Noguchi, H.; Hoshina, T.; Takahashi, T.; Kodama, N.; Tsurumi, T. Calcium aluminate silicate $Ca_2Al_2SiO_7$ single crystal applicable to piezoelectric sensors at high temperature. *Appl. Phys. Lett.* **2013**, *102*, 242907. [CrossRef]

15. Shen, C.; Zhang, S.; Cao, W.; Cong, H.; Yu, H.; Wang, J.; Zhang, H. Thermal and electromechanical properties of melilite-type piezoelectric single crystals. *J. Appl. Phys.* **2015**, *117*, 064106. [CrossRef]

16. Yaokawa, R.; Kimura, H.; Aota, K.; Uda, S. Precipitation phenomena in and electrical resistivity of high-temperature treated langatate ($La_3Ta_{0.5}Ga_{5.5}O_{14}$). *IEEE Trans. Ultra. Ferro. Freq. Contr.* **2011**, *58*, 1131–1139. [CrossRef] [PubMed]

17. Spassky, D.A.; Kozlova, N.S.; Kozlova, A.P.; Zabelina, E.V.; Buzanov, O.A.; Buryi, M.; Laguta, V.; Lebbou, K.; Nehari, A.; Cabane, H.; et al. Study of the defects in $La_3Ta_{0.5}Ga_{5.5}O_{14}$ single crystals. *J. Lumin.* **2016**, *180*, 95–102. [CrossRef]

18. Takahashi, I.; CITIZEN FINEDEVICE CO., LTD, Fujikawaguchiko-Machi, Yamanashi, Japan. Personal communication, 2019.

19. Kasano, H.; Hara, T.; Minakuchi, Y. Thermal stress (Netsuouryoku). In *Fundamental of Mechanics of Materials (Kisozairyorikigaku)*, 1st ed.; Koizumi, T., Ed.; Yokendo: Tokyo, Japan, 2014; pp. 30–33. (In Japanese)

20. Wang, Z.; Cheng, X.; Yuan, D.; Pan, L.; Guo, S.; Xu, D.; Lv, M. Crystal growth and properties of $Ca_3NbGa_3Si_2O_{14}$ single crystals. *J. Cryst. Growth* **2003**, *249*, 240–244. [CrossRef]

21. Takeda, H.; Sato, J.; Kato, T.; Kawasaki, K.; Morikoshi, H.; Shimamura, K.; Fukuda, T. Synthesis and characterization of $Sr_3TaGa_3Si_2O_{14}$ single crystals. *Mater. Res. Bull.* **2000**, *35*, 245–252. [CrossRef]

22. Shi, X.; Yuan, D.; Yin, X.; Wei, A.; Guo, S.; Yu, F. Crystal growth and dielectric, piezoelectric and elastic properties of $Ca_3TaGa_3Si_2O_{14}$ single crystal. *Solid State Commun.* **2007**, *142*, 173–176. [CrossRef]

23. Usui, H.; Kusakabe, H.; Tokuda, M.; Sugiyama, K.; Hoshina, T.; Tsurumi, T.; Takeda, H. Structure and electrical properties of $Ba_3TaGa_3Si_2O_{14}$ single crystals grown by Czochralski method. *J. Ceram. Soc. Jpn.* **2020**, *128*, 441–446. [CrossRef]

24. Karaki, T.; Sato, R.; Adachi, M.; Kushibiki, J.; Arakawa, M. Piezoelectric properties of $Ca_3NbGa_3Si_2O_{14}$ single crystal. *Jpn. J. Appl. Phys.* **2004**, *43*, 6721–6724. [CrossRef]

25. Fu, X.; Víllora, E.G.; Matsushita, Y.; Kitanaka, Y.; Noguchi, Y.; Miyayama, M.; Shimamura, K.; Ohashi, N. Piezoelectric $Ca_3TaAl_3Si_2O_{14}$ (CTAS): High quality 2-in. single-crystal growth and electro-elastic properties from room to high (650 °C) temperature. *J. Cryst. Growth* **2018**, *501*, 38–42. [CrossRef]

26. Takeda, H.; Kato, T.; Chani, V.I.; Morikoshi, H.; Shimamura, K.; Fukuda, T. Effect of (Sr, Ba) substitution in $La_3Ga_5SiO_{14}$ and $La_3M_{0.5}Ga_{5.5}O_{14}$ (M = Nb^{5+}, Ta^{5+}) crystals on their synthesis, structure and piezoelectricity. *J. Alloys Compd.* **1999**, *290*, 79–84. [CrossRef]

27. ANSI/IEEE Std 176. *IEEE Standard on Piezoelectricity*; IEEE: New York, NY, USA, 1987.

28. Ikeda, T. *Fundamentals of Piezoelectricity*; Oxford University Press: New York, NY, USA, 1990.

29. Chilla, E.; Flannery, C.M.; Frohlich, H.-J.; Straube, U. Elastic properties of langasite-type crystals determined by bulk and surface acoustic waves. *J. Appl. Phys.* **2001**, *90*, 6084–6091. [CrossRef]

30. Beaucage, T.R.; Beenfeldt, E.P.; Speakman, S.A.; Porter, W.D.; Payzant, E.A.; Pereira Da Cunha, M. Comparison of high temperature crystal lattice and bulk thermal expansion measurements of LGT single crystal. In Proceedings of the 2006 IEEE International Frequency Control Symposium and Exposition, Miami, FL, USA, 4–7 June 2006; pp. 658–663.

31. Shannon, R.D. Revised effective ionic radii and systematic studies of interatomic distances in halides and chalcogenides. *Acta Crystallogr. A* **1976**, *32*, 751–766. [CrossRef]

32. Bohm, J.; Chilla, E.; Flannery, C.; Frohlich, H.-J.; Hauke, T.; Heimann, R.B.; Hengst, M.; Straube, U. Czochralski growth and characterization of piezoelectric single crystals with langasite structure: $La_3Ga_5SiO_{14}$ (LGS), $La_3Ga_{5.5}Nb_{0.5}O_{14}$ (LGN) and $La_3Ga_{5.5}Ta_{0.5}O_{14}$ (LGT) II. Piezoelectric and elastic properties. *J. Cryst. Growth* **2000**, *216*, 293–298. [CrossRef]

33. Trolier-McKinstry, S.; Cross, L.E.; Yamashita, Y. (Eds.) *Piezoelectric Single Crystals and Their Applications*; Pennsylvania State University: University Park, PA, USA, 2004.

Publisher's Note: MDPI stays neutral with regard to jurisdictional claims in published maps and institutional affiliations.